A substructured FE/XFE method for stress intensity factors computation in an industrial structure

Eric Wyart[*] **– Danielle Coulon**[*] **– Philippe Martiny**[*]
Thomas Pardoen[**] **– Jean-François Remacle**[***] **– Frédéric Lani**[*]

[*] *Cenaero*
Rue Jean Mermoz 30
B-6041 Gosselies

[**] *Department of Material Science and Processes*
Université catholique de Louvain
B-1348 Louvain-la-Neuve

[***] *Department of Civil Engineering*
Université catholique de Louvain
B-1348 Louvain-la-Neuve

eric.wyart@cenaero.be

ABSTRACT. *The introduction of the* eXtended Finite Element Method *(*X-FEM*) into a commercial* Finite Element *(*FE*) software was achieved through a substructuring method. For fracture mechanics problems, the domain is decomposed into cracked and safe subdomains which are solved by the XFE-code and the FE-software, respectively. The interface problem is solved using a* FETI *solver. The new approach is compared with a classical* FE*-approach in the case of a planar crack in a compressor drum of a turbofan engine.*

RÉSUMÉ. *La* méthode des éléments finis étendus *(notée* X-FEM*) a été introduite dans un code* Eléments Finis *(*EF*) commercial par une méthode de sous-structuration. L'approche consiste à diviser la géométrie en sous-domaines sains et fissurés, traités respectivement par un logiciel* EF *commercial et par un code basé sur la formulation* X-FEM. *Le problème d'interface entre les sous-domaines est résolu par la méthode* FETI. *Cette contribution compare les méthodes éléments finis classiques et étendus appliquées au cas d'une pièce de moteur d'avion fissurée.*

KEYWORDS: *X-FEM,* level set, *FETI, substructuring method, domain decomposition.*

MOTS-CLÉS : *X-FEM,* level set, *FETI, méthode de sous-structuration, décomposition de domaine.*

REMN – 16/2007. X-FEM, pages 199 to 212

1. Introduction

In the last decade the *eXtended Finite Element Method* (*X-FEM*) (Moës *et al.*, 1999) has been developed in order to solve singularity and/or discontinuity problems without the need of building conforming mesh.

The *X-FEM* is particularly suited for Fracture Mechanics problems as it leads to a satisfactory evaluation of the stress intensity factors and provides realistic crack paths with no or minimal remeshing. The method is thus expected to be widely used in the near future by some of the major players of the aeronautics sector interested for instance in the numerical prediction of the total fatigue life of complex geometries.

However, the method involves several specific features (formulation, use of level sets...) and its implementation could require important modifications of the kernel of the most common General Purpose Finite Element Software used by the industrial majors. Therefore, several strategies have been proposed which allow for the use of the X-FEM in commercial FE-software through available connections such as user-defined elements, super-elements (Bordas *et al.*, 2006; Wyart *et al.*, 2006)...

Recently a *Substructured Finite Element/eXtended Finite Element method* (*S-FE/XFE*) (Wyart *et al.*, 2006) has been proposed. The method consists in decomposing the domain into a FE-domain and a XFE-domain. The interface problem between the two subdomains is solved using the *Finite Element Tearing and Interconnecting* (*FETI*) method.

In this contribution, the *S-FE/XFE* method is applied to an industrial application of a cracked section of the compressor drum of an airplane engine submitted to centrifugal forces. Results obtained with the *S-FE/XFE* method and with a conforming *Finite Element Method* (*FEM*) are compared in terms of:

– accuracy of the stress intensity factors,

– mesh convergence,

– user's operations,

– total computational and user time.

Section 2 provides the basis of the *X-FEM* and the *level set method*. The *S-FE/XFE* is explained in Section 3. Finally, the application is presented and commented in Section 4.

2. Theoretical background

2.1. *Extended Finite Element Method (X-FEM)*

The *eXtended Finite Element Method* (*X-FEM*) (Moës *et al.*, 1999) is based on the *partition of unity method* (Melenk *et al.*, 1996). The *X-FEM* allows for introducing an *a priori* knowledge of the solution in a local region into the FE-formulation. As

a consequence of the *partition of unity method*, conforming meshes are not required. Considering fracture mechanics problems, the approximation of the displacement field in the *XFEM* can be written as

$$\boldsymbol{u}^h(\mathbf{x}) = \sum_{i\in I} \boldsymbol{u}_i \phi_i(\mathbf{x}) + \sum_{j\in J} \boldsymbol{b}_j \phi_j(\mathbf{x}) H(\mathbf{x}) + \sum_{k\in K} \phi_k(\mathbf{x}) \sum_{l=1}^{4} \boldsymbol{c}_k^l F^l(\mathbf{x}) \qquad [1]$$

where

– ϕ_i is the shape function associated to node i,

– I is the set of all nodes of the domain,

– J is the set of nodes whose shape functions support is cut by a crack,

– K is the set of nodes whose shape functions support contains the crack front,

– $\boldsymbol{u}_i$ are the classical degrees of freedom (*i.e.* displacement) for node i,

– $\boldsymbol{b}_j$ account for the jump in the displacement field across the crack at node j. If the crack is aligned with the mesh, $\boldsymbol{b}_j$ represents the opening of the crack,

– $H(\mathbf{x})$ is the Heaviside function,

– $\boldsymbol{c}_k^l$ are the additional degrees of freedom associated with the crack tip enrichment functions F^l,

– F^l is an enrichment which corresponds to the four asymptotic functions in the development expansion of the crack tip displacement field in a linear elastic solid (Moës *et al.*, 1999).

2.2. *Level set method*

As proposed in (Stolarska *et al.*, 2001), the *level set method* (Sethian, 1996) is used for modelling cracks. A crack is described by two *level sets* (see Figure 1):

(i) a normal *level set*, $\psi_n(\mathbf{x})$, *i.e.* the signed distance to the crack surface,

(ii) a tangent *level set* $\psi_t(\mathbf{x})$, *i.e.* the signed distance to the plane including the crack tip and perpendicular to the crack surface.

The *level sets* are used for two different purposes:

– determining which nodes must be enriched,

– defining the domain decomposition.

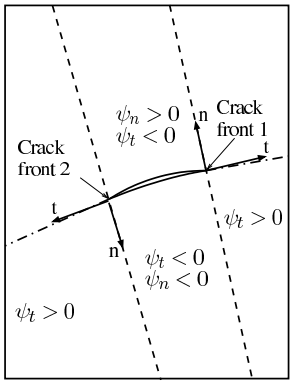

- ψ_n: normal level set,
  i.e. the signed distance from the crack surface
- ψ_t: tangent level set,
  i.e. the signed distance from the plane including
  the crack front and perpendicular to the crack surface

Figure 1. *Representation of a crack by two* level sets *($\psi_n(\mathbf{x})$ and $\psi_t(\mathbf{x})$)*

3. Substructured FE/XFE method (S-FE/XFE)

3.1. *Introduction*

Coupling the *X-FEM* with a FE-code by means of a substructuring method was first proposed by (Bordas *et al.*, 2006). In this method, the FE-domain is treated as a super-element. The degrees of freedom and the right hand side of the FE-domain are reduced on the boundary of the XFE-domain.

Recently (Wyart *et al.*, 2006) introduced the *Finite Element Tearing and Interconnecting* method (Farhat *et al.*, 1991) for solving the interface problem between XFE- and FE-domains for 3D problems. This approach is referred here to as the *substructured FE/XFE* method (*S-FE/XFE*).

The global algorithm is presented next. Details about the domain decomposition and the *FETI* method are given in Subsections 3.3 and 3.4.

3.2. *Global algorithm*

In a *S-FE/XFE* problem, the whole domain is divided into two subdomains:

– the FE-domain (treated by the FE-software[1].),

– the XFE-domain (treated be the XFE-code).

For each element of a subdomain, the elementary stiffness matrix and the localization of the degrees of freedom in the global stiffness matrix (called “locel”) are

1. In our case SAMCEF^{TM} (SAMCEF, 2006).

computed and written in a binary file. These information are read by the FETI-code[2] which assembles the local stiffness matrices and solves the global interface system. Finally, the solution is transfered back to the S-FE/XFE library that computes the stress intensity factors by the *equivalent domain integral* method (*EDI*) (Moran *et al.*, 1987). The *equivalent domain integral* method is based on the *interaction integral* method (Yau *et al.*, 1980).

The global resolution algorithm is shown in Figure 2.

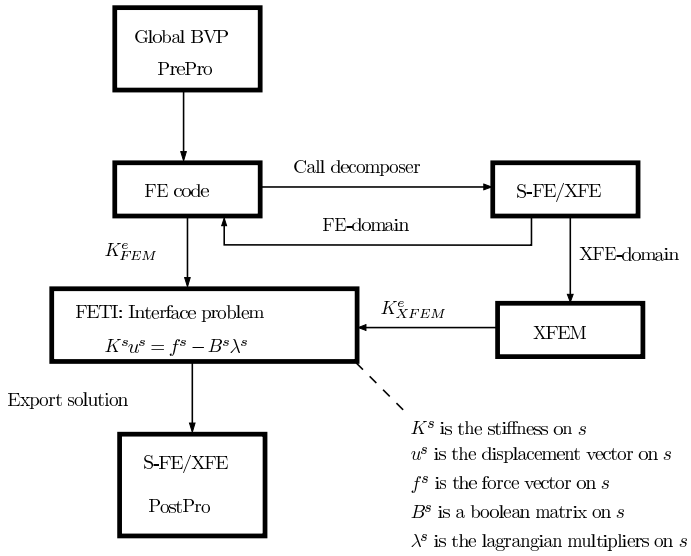

Figure 2. *Communications between the FETI solver, the* host *FE-code and the S-FE/XFE library for a boundary value problem (BVP)*

3.3. *Domain decomposition*

The decomposition is based on the *level set* value. The size of the XFE-domain is such that the *EDI* belongs to the XFE-domain. The interface of the subdomain *cannot include enriched degrees of freedom* in order to ensure the compatibility between the FE- and the XFE-domains as the FE-software can not deal with enriched degrees fo freedom. This kind of decomposition minimizes the computation time of the matrix generation on the XFE-domain which is sequential. Consequently, the computational load is not properly balanced between the processor dealing with the FE-domain and the processor attributed to the XFE-domain.

2. The FETI-code has been developped by François-Xavier Roux from the ONERA. It is used in the frame of a collaboration with SAMTECH.

3.4. *FETI*

In this subsection, we recall briefly the basic mathematical concepts of the *FETI* method.

The *FETI* method has been developed to handle and solve large scale problems. *FETI* allows both parallel and sequential computation schemes. According to (Lesoinne *et al.*, 1998), computational time and memory requirements are respectively one to two orders of magnitude lower than those of a direct solver. The whole domain is divided into several substructures. The problem is reduced to an interface problem.

Let us consider a domain Ω. The condition of static equilibrium is written as

$$\mathbf{K}\mathbf{u} = \mathbf{f} \qquad [2]$$

where $\mathbf{K}$ is the stiffness matrix (symmetric semi-definite positive) on the domain Ω, $\mathbf{u}$ is the nodal displacement vector and $\mathbf{f}$ is the force vector. The domain Ω is divided into N_s non-overlapping subdomains Ω_s. The *FETI* method consist in replacing Equation [2] by

$$\mathbf{K}^{(s)}\mathbf{u}^{(s)} = \mathbf{f}^{(s)} - \mathbf{B}^{(s)T}\boldsymbol{\lambda} \qquad \text{with} \quad s = 1, \cdots, N_s; \qquad [3]$$

$$\Delta = \sum_{s=1}^{N_s} \mathbf{B}^{(s)}\mathbf{u}^{(s)} = \mathbf{0}, \qquad [4]$$

where $\mathbf{K}^{(s)}$ and $\mathbf{f}^{(s)}$ are the contributions from the subdomain $\Omega^{(s)}$ respectively to $\mathbf{K}$ and $\mathbf{f}$, $\boldsymbol{\lambda}$ is a vector of Lagrange multipliers and $\mathbf{B}^{(s)}$ is a signed boolean matrix that accounts for the localization of the degrees of freedom on the interface.

Lagrange multipliers are introduced to enforce continuity of the displacements on the boundary $\Gamma^{(s)}$ of the subdomain (*i.e.* $\Delta = \mathbf{0}$ on $\Gamma^{(s)}$). Generally, a mesh partition can contain $N_f \leq N_s$ floating substructures (*i.e.* substructures with an insufficient number of essential boundary conditions to avoid kinematic modes in the matrix $\mathbf{K}^{(s)}$).

The general solution for a floating subdomain is given by

$$\mathbf{u}^{(s)} = \mathbf{K}^{(s)+}(\mathbf{f}^{(s)} - \mathbf{B}^{(s)T}\boldsymbol{\lambda}) + \mathbf{R}^{(s)}\boldsymbol{\alpha}^{(s)} \qquad [5]$$

where $\mathbf{K}^{(s)+}$ is a generalized inverse of $\mathbf{K}^{(s)}$, $\mathbf{R}^{(s)} = \text{Ker}(\mathbf{K}^{(s)})$ is the kernel of $\mathbf{K}^{(s)}$ (rigid body modes) and $\boldsymbol{\alpha}$ is a vector containing a maximum of six constants which account for the six possible kinematic modes. Equation [3] admits a solution if and only if its right hand side is orthogonal to $Ker(\mathbf{K}^{(s)})$. This statement means that the forces cannot excite the rigid modes of the subdomain. These considerations lead to the interface problem:

$$\begin{bmatrix} \mathbf{F_I} & -\mathbf{G_I} \\ -\mathbf{G_I}^T & \mathbf{0} \end{bmatrix} \begin{bmatrix} \boldsymbol{\lambda} \\ \boldsymbol{\alpha} \end{bmatrix} = \begin{bmatrix} \mathbf{d} \\ -\mathbf{e} \end{bmatrix} \qquad [6]$$

where

$$\begin{aligned}
\mathbf{F_I} &= \sum_{s=1}^{N_s} \mathbf{B}^{(s)}\mathbf{K}^{(s)+}\mathbf{B}^{(s)T}; \\
\mathbf{G_I} &= [\ \mathbf{B}^{(1)}\mathbf{R}^{(1)} \quad \cdots \quad \mathbf{B}^{(N_f)}\mathbf{R}^{(N_f)}\ ]; \\
\boldsymbol{\alpha}^T &= [\ \boldsymbol{\alpha}^{(1)T} \quad \cdots \quad \boldsymbol{\alpha}^{(N_f)T}\ ]^T; \\
\mathbf{d} &= \sum_{s=1}^{N_s} \mathbf{B}^{(s)}\mathbf{K}^{(s)+}\mathbf{f}^{(s)}; \\
\mathbf{e}^T &= [\ \mathbf{R}^{(1)}\mathbf{f}^{(1)T} \quad \cdots \quad \mathbf{R}^{(N_f)}\mathbf{f}^{(N_f)T}\ ]^T.
\end{aligned} \qquad [7]$$

The global interface problem is solved by a *Projected Conjugate Gradient* method (*PCG*) (Saad, 2000). For more details, see again (Farhat *et al.*, 1994).

4. Numerical application

The *S-FE/XFE* method is applied to a crack analysis in a section of a compressor drum of a turbofan engine. The results obtained with the *S-FE/XFE* method are compared with those obtained with a standard FE computation. The standard FE problem is solved using the *FETI* method with the same decomposition as the S-FE/XFE problem in order to assess the influence of the *X-FEM* on the solver behaviour. The influence of mesh refinement at the crack tip is studied. The initial mesh is chosen so as to ensure convergence of the strain energy for the non-cracked standard FE problem.

4.1. *Description*

Most modern airliners are equipped with turbofan engines. Generally, these consist from upstream to downstream direction, of an air intake, a fan, a low-pressure compressor, a high-pressure compressor, a combustion chamber, a high-pressure turbine, a low-pressure turbine, a mixing duct and a nozzle. Axial compressors and turbines are divided into several stages, each one being made of a rotor, or bladed disc, and a stator or bladed shroud. When assembled together, the bladed discs of a compressor or of a turbine form what is referred to as a drum.

The particular structure which is studied in this paper is a drum of a low pressure compressor. It is schematically depicted in Figure 3, showing three distinct flanges. The flange located far upstream is meant to be bolted with the fan disc while the two other flanges accommodate circular plates sealing up the air duct.

To limit the problem to a reasonable computational size, the drum is arbitrarily cut in the transverse direction, before the first compressor stage.

The part of the drum simulated in this application is shown in Figure 4. Only an angular section of this part is used for the computation owing to axial symmetry.

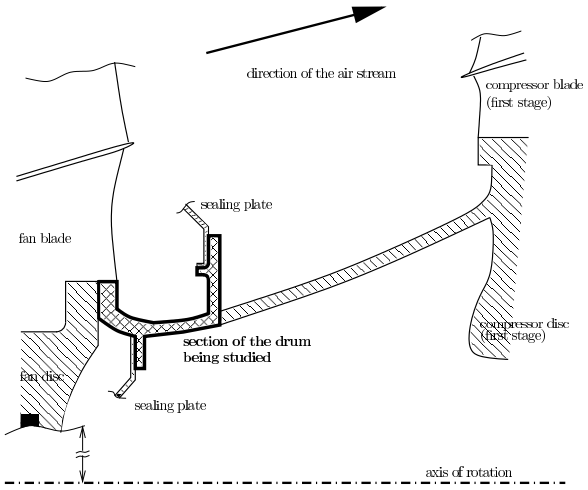

Figure 3. *Schematic view of the compressor drum*

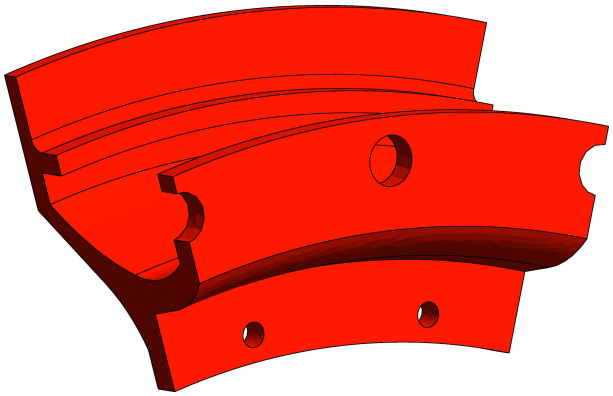

Figure 4. *Section of the drum studied in this work*

4.2. *Loading and boundary conditions*

The drum is submitted to centrifugal forces $\mathbf{f}_c$ given per unit volume by

$$\mathbf{f}_c = -\rho(\boldsymbol{\omega} \times (\boldsymbol{\omega} \times \mathbf{r})) \qquad [8]$$

where $\boldsymbol{\omega}$ is the rotation speed vector and $\mathbf{r}$ is the position vector related to the rotation axis.

Periodic boundary conditions are imposed in order to represent the rotational symmetry of the drum. The axial displacement is fixed on the upper exterior holes.

4.3. *Computation sequences*

The computation sequences for the standard FE and the Substructured FE/XFE crack problems are explained hereafter.

4.3.1. *Crack definition*

A through-thickness crack is inserted into the model at the center hole of the structure. The direction of the crack is radial. The crack is shown in Figure 5.

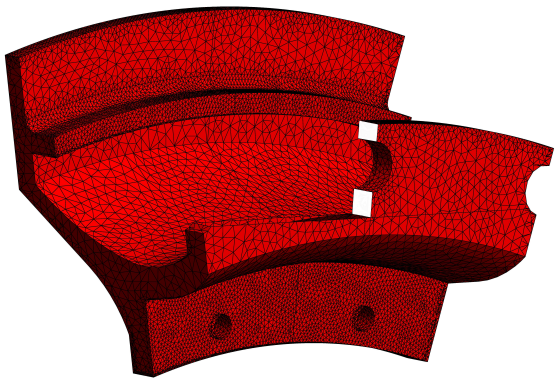

Figure 5. *Crack representation (in white) in the drum*

There are two different methods for introducing the crack depending on the method used:

– standard *FEM*: the crack is introduced into the CAD by inserting a closed surface leading to a renumbering of all the geometrical entities of the CAD[3]. The related data (materials, boundary conditions...) must be updated due to the modification of the CAD;

– *S-FE/XFE* method: the crack is introduced by means of its *level sets*. The CAD is not modified and the previous dataset can be used without any changes.

3. It depends on the software used for generating the CAD model and the mesh.

4.3.2. *Mesh generation*

In the standard *FEM* case, the mesh generation is decomposed in two steps:

– the mesh is generated on the whole domain and the crack surface is also meshed,

– the nodes on the crack surface are duplicated and the mesh is splitted.

For the *S-FE/XFE* method, the mesh is arbitrarily generated on the whole domain.

The mesh has been refined at the crack tip in both cases in order to improve the accuracy of the solution at the crack tip. Mesh adaptation during the computation has not been considered in this work.

4.3.3. *Elementary stiffness generation*

The elementary stiffness generation for the *S-FE/XFE* method is made by both the FE-software and the XFE-code (see Figure 2)[4]. The time spent during this step depends on the size of the XFE-domain. For the standard *FE* problem, the elementary stiffness matrices are only created by the FE-software.

The different steps are summarized in the Table 1 for both standard *FE* and *S-FE/XFE* methods.

Table 1. *Computation sequences for* FE *and* S-FE/XFE *methods*

Step	Standard *FE*	*substructured FE/XFE*
CAD	Introduction of the crack surface	Nothing to do
Meshing	Duplicate nodes and split the mesh on the crack face and mesh refinement at crack tip (optional)	Mesh refinement at crack tip (optional)
Computing	Elementary stiffnesses generation by the FE-software and calling of the FETI solver	Mesh decomposition in two subdomains (FE-domain and XFE-domain) and generation of the elementary stiffnesses by the FE-software, the XFE-code and calling the FETI solver
SIF	Result recovery and computation of the stress intensity factor by the *EDI* method	Result recovery and computation of the stress intensity factor by the *EDI* method

4. Currently, this step is sequential.

4.4. *Results*

Figure 6 shows the variation of the mode I stress intensity factors K_I as a function of the number of degrees of freedom. These values are obtained for various level of mesh discretisation at the crack tip. The accuracy of the stress intensity factors is obviously improved when increasing the number of degrees of freedom. The first point corresponds to the original mesh size. With the original mesh, the error calculated from the difference to the converged solution (*i.e.* number of degrees of freedom $> 1.8 \cdot 10^5$) is equal to only 1.7% with the *S-FE/XFE* while it is equal to 4.8% with the standard *FE* method.

A *S-FE/XFE* computation without the crack tip enrichment functions has been performed on the original mesh in order to demonstrate the influence of the crack tip enrichment on the results accuracy. In this case, the error on the SIF estimation is equal to 6.3%. This result shows the important effect of introducing the *linear elastic fracture mechanics* solution into the shape function space at the crack tip.

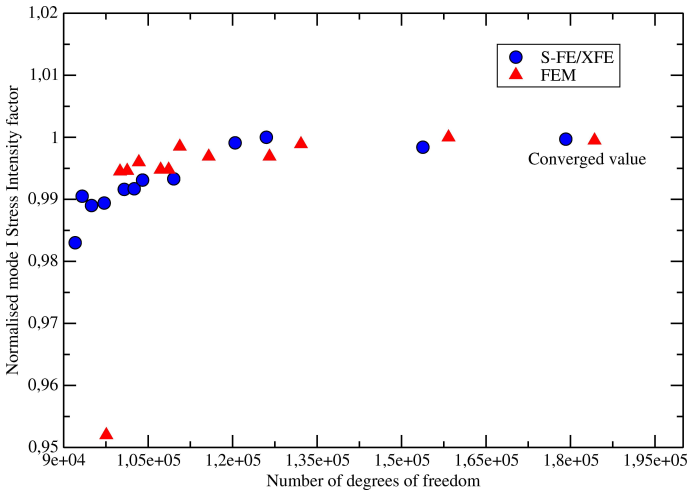

Figure 6. *Comparison of the mode I stress intensity factor for both the* FE *and* S-FE/XFE method

4.5. *Discussion*

The FE and FE/XFE results are compared in terms of:

– mesh convergence,

– influence of the *X-FEM* on *Projected Conjugate Gradient* algorithm convergence,

– user's operations,

– total computational and user time.

4.5.1. *Mesh convergence*

The first interesting result concerning the *S-FE/XFE* method with crack tip enrichment functions is the relatively good approximation of the stress intensity factor using the initial mesh[5]. As expected, the two methods converge to the same values after some degree of refinement at the crack tip.

4.5.2. *Influence of the method on the resolution of the local and the global problems*

As the crack is not close to the interface, the number of iteration of the *PCG* algorithm is essentially governed by the size of the interface. The number of iterations is not influenced by the presence of enriched degrees of freedom. Because the XFE-domain is smaller than the FE-domain, as shown Figure 7, the time associated to the *FETI* solver depends on the FE-domain size. Decomposing the FE-domain itself into several safe subdomains will lead to a decrease of the global computational time which might then become essentially dependent of the XFE-domain size.

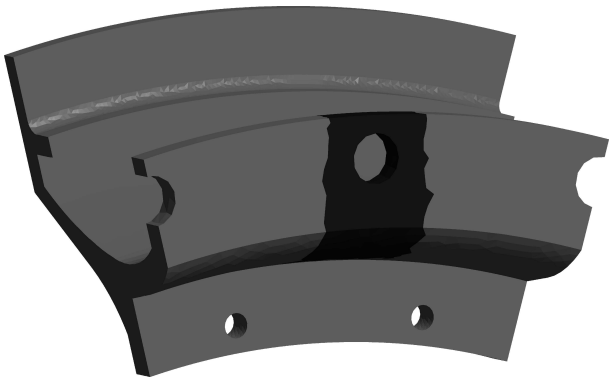

Figure 7. *Mesh decomposition of the drum, in dark grey the XFE-domain in light grey the FE-domain*

4.5.3. *User's operations*

Compared to the *S-FE/XFE* method, the *FE* method requires more user's interventions. First the original CAD must be modified by inserting a crack surface. The main consequence is the renumbering of the geometrical entities. Hence, all the data must be modified in order to apply the boundary conditions and the material characteristics at the proper location. This operation can take a lot of time depending on the

5. This result must be taken in its context. A convergence study or an estimation of the error must always be done in order to verify the validity of the result.

complexity of the geometry, the quality of the original CAD, the experience of the user.

4.5.4. *General discussion on the total computational time*

In order to reduce the design and analysis cost, mechanical engineers and software designers:

– tend to develop tools which avoid time-consuming user related operations,

– continuously improve the computational efficiency of existing tools.

As explained here above, the *S-FE/XFE* approach limits the number of interventions of the user and significantly simplifies the "mesh generation" task. This is of the utmost importance in today's industrial design and analysis process. Indeed, following (Hughes, 2004), "mesh generation" is attributed to taking over 80% of all analysis time in major engineering industries such as shipbuilding, aerospace and automotive. It has become the major bottleneck in engineering analysis.

However, for what concerns the remaining computational time (CAD operations and mesh generation excluded), the *S-FE/XFE* method is, for the same mesh refinement level, globally slightly slower due to the time spent on mesh decomposition and matrix generation on the XFE-domain.

5. Conclusions and prospects

The *Substructured Finite Element/eXtended Finite Element* method has been applied to an industrial structure and proved to be competitive with a conformly meshed crack solved by the *Finite Element Method*. The two methods converge to the same mode I stress intensity factors. The user time, which is critical for the industry, is clearly reduced due to the fact that:

– the "Computer Aided Design" does not need to be changed,

– the mesh generation is significantly simplified.

Nevertheless, the computational time is slightly increased by the mesh decomposition and the elementary stiffness generation.

The interface between the FE-domain and the XFE-domain can not include enriched degrees of freedom as these are obviously not handled by the FE-software. While the introduction of the enrichment functions modifies the conditioning of the XFE-domain stiffness matrix, it does not influence the convergence of the *Projected Conjugate Gradient* solving the condensated problem at the interface (where the unknowns are the lagrange multipliers).

The *Substructured Finite Element/eXtended Finite Element* method with crack tip enrichment functions has shown to give a good approximation of the mode I stress intensity factor for the coarser mesh where the *Finite Element Method* leads to much cruder approximation.

The *Substructured Finite Element/eXtended Finite Element* method is currently being extended to the coupling of *Finite Element*-shell and *eXtended Finite Element*-3D formulations. This extension opens new areas of investigation such as the delamination of composite materials.

6. References

Bordas S., Moran B., « Enriched Finite Elements and Level Sets for Damage Tolerance Assessment of Complex Structures », *Engineering Fracture Mechanics*, 2006. in press.

Farhat C., Roux F. X., « A Method of Finite Element Tearing and Interconnecting and its Parallel Solution Algorithm », *International Journal for Numerical Methods in Engineering*, vol. 32, p. 1205-1227, 1991.

Farhat C., Roux F. X., « Implicit Parallel Processing in Structural Mechanics », *Computational Mechanical Advance*, vol. 2, n° 1, p. 1-124, 1994. North-Holland.

Hughes T., « Consider a Spherical Cow- Conservation of Geometry in Analysis: Implications for Computational Methods in Engineering », *IMA Workshop: Compatible Spatial Discretizations for Partial Differential Equations*, 2004.

Lesoinne M., Pierson K., « An efficient FETI implementation on distributed shared memory machine with independent numbers of subdomains and processors », *Contemporary Mathematics*, 1998.

Melenk J. M., Babuška I., « The Partition of Unity Finite Element Method: Basic Theory and Applications », *Computer Methods in Applied Mechanics and Engineering*, vol. 139, p. 289-314, 1996.

Moës N., Dolbow J., Belytschko T., « A finite element method for crack growth without remeshing », *International Journal for Numerical Methods in Engineering*, vol. 46, p. 131-150, 1999.

Moran B., Shih C. F., « Crack Tip and Associated Domain Integrals from Momentum and Energy Balance », *Engineering Fracture Mechanics*, vol. 27, n° 6, p. 615-641, 1987.

Saad Y., *Iterative methods for sparse linear systems*, 2nd edn, SIAM, 2000.

SAMCEF, General purpose finite element analysis package, Technical report, http://www.samcef.com, 2006.

Sethian J. A., *Level Set Methods and Fast Marching Methods: Evolving Interfaces in Computational Geometry, Fluid Mechanics, Computer Vision, and Material Science*, Cambridge University Press, Cambridge, 1996.

Stolarska M., Chopp D. L., Moës N., Belytschko T., « Modelling Crack Growth by Level Sets in the Extended Finite Element Method », *International Journal for Numerical Methods in Engineering*, vol. 51, p. 943-960, 2001.

Wyart E., Dufbt M., Coulon D., Martiny P., Pardoen T., Remacle J.-F., Lani F., « Substructuring FE-XFE approaches applied to three dimensional crack propagation », *Submitted to the Journal of Computational and Theoretical Applied Mathematics*, 2006.

Yau J. F., Wang S. S., Corten H. T., « A Mixed-Mode Crack Analysis of Isotropic Solids Using Conservation Laws of Elasticity », *Journal of Applied Mechanics*, vol. 47, p. 335-341, 1980.